

The hard segment unit cell for MDI-BDO-based polyurethane elastomers

J. R. Quay*, Z. Sun and J. Blackwell†

Department of Macromolecular Science, Case Western Reserve University, Cleveland, OH 44106, USA

and R. M. Briber‡ and E. L. Thomas§

Department of Polymer Science, University of Massachusetts, Amherst, MA 00103, USA
(Received 20 October 1988; revised 19 May 1989; accepted 1 July 1989)

X-ray and electron diffraction data have been combined to determine the unit cell for the hard domains of 4,4'-diphenylmethane diisocyanate/butanediol-based polyurethane elastomers. The analysis has been aided by manipulating digital intensity data obtained from two-dimensional densitometer scans of the diffraction patterns. A total of 22 reflections are resolved in the electron diffraction patterns, of which 11 are detected by X-rays. The unit cell is triclinic with dimensions $a=5.33$, $b=5.26$, $c=38.68$ Å, $\alpha=113.6$, $\beta=116.0$, $\gamma=94.4^\circ$. The reflections in the X-ray fibre diagrams of stretched annealed film are displaced above and below the apparent layer lines, which points to inclination of the chain axis (c) away from the direction of the draw. Refinement of coordinates of the predicted reflections shows that the c axis is tilted by 2.5° away from the direction of draw, approximately in the $\bar{1}11$ plane.

(Keywords: polyurethanes; X-ray diffraction; electron diffraction; elastomers)

INTRODUCTION

Polyurethane elastomers are block copolymers composed of alternating 'hard' urethane and 'soft' polyether or polyester segments. Their elastomeric properties derive from the phase separation¹ of the urethane blocks to form hard domains that act as physical crosslinks and as filler particles within the soft segment matrix. We are studying the structure of systems in which the urethane blocks are formed from 4,4'-diphenylmethane diisocyanate (MDI) and 1,4-butanediol (BDO). These have been shown by X-ray diffraction studies to form semicrystalline hard domains^{2,3}. Since many of the properties of the elastomers, especially at higher temperatures, depend on the chemistry of the hard segments, there is considerable interest in the structure and morphology of these domains.

Figure 1a shows the X-ray fibre diffraction pattern for a MDI-BDO-based polyurethane elastomer containing $\approx 50\%$ hard segments, in which the soft segments are poly(tetramethylene adipate) ($M_n=2000$). The specimen had been oriented by stretching 700% and then annealed at 130°C for 7d. Annealing eliminates soft segment crystallinity and increases the crystallinity, crystallite size and crystalline perfection of the hard domains. The diffraction pattern contains 11 independent Bragg reflections, all of which have been assigned to the hard domains. A schematic diagram of the pattern is shown in Figure 1b, in which the reflections are numbered for

reference below. The absence of row lines and the angular grouping of reflections is indicative of triclinic symmetry for the unit cell. As is typical of semicrystalline polymers, the reflections are broad and arced due to the small crystallite size and imperfect orientation of the chains parallel to the direction of draw. In addition, the non-crystalline regions of the sample size rise to a broad halo at $d=4.5$ Å \parallel , which tends to obscure the reflections.

Blackwell and Ross⁴ were able to index the 11 observed reflections with a triclinic unit cell with dimensions $a=5.05$, $b=4.67$, $c=37.9$ Å, $\alpha=116$, $\beta=116$ and $\gamma=83.5^\circ$. It was later suggested⁵ that some of the reflections in Figure 1, notably the reflection at $d=4.9$ Å, may be due to the presence of a second polymorphic form. Evidence for polymorphism in these polymers has been reported in X-ray⁶, differential scanning calorimetry (d.s.c.)⁶ and electron microscopy^{7,8} studies. Electron diffraction analysis of different polymorphs effectively demonstrated that the 4.9 Å reflection is due to a second structure with a shorter fibre repeat. The remaining reflections can be indexed by a unit cell with the same dimensions except for $a=b=5.05$ Å. However, the theoretical densities for these proposed unit cells are 1.58 and 1.42 g cm⁻³, respectively, and these figures are both unreasonably high compared with the reported densities for homopoly-(MDI-BDO), which range from 1.25 to 1.35 g cm⁻³ (References 9 and 10). Born *et al.*⁹ have proposed a unit cell with dimensions $a=4.92$, $b=5.66$, $c=38.35$ Å, $\alpha=124$, $\beta=104.5$ and $\gamma=86^\circ$. This has a calculated density of 1.32 g cm⁻³, which is in much better agreement with the observed value. However, this unit cell is only able to index 8 of the 11 reflections, one of which is that at $d=4.9$ Å, now assigned to the second polymorph.

Insight into the chain conformation and packing of

$\parallel 1 \text{ \AA} = 10^{-1} \text{ nm}$

* Current address: Air Products and Chemicals, Allentown, PA 18105, USA

† To whom correspondence should be addressed

‡ Current address: National Bureau of Standards, Gaithersburg, MD 20899, USA

§ Current address: Department of Materials Science, Massachusetts Institute of Technology, Cambridge, MA 02139, USA

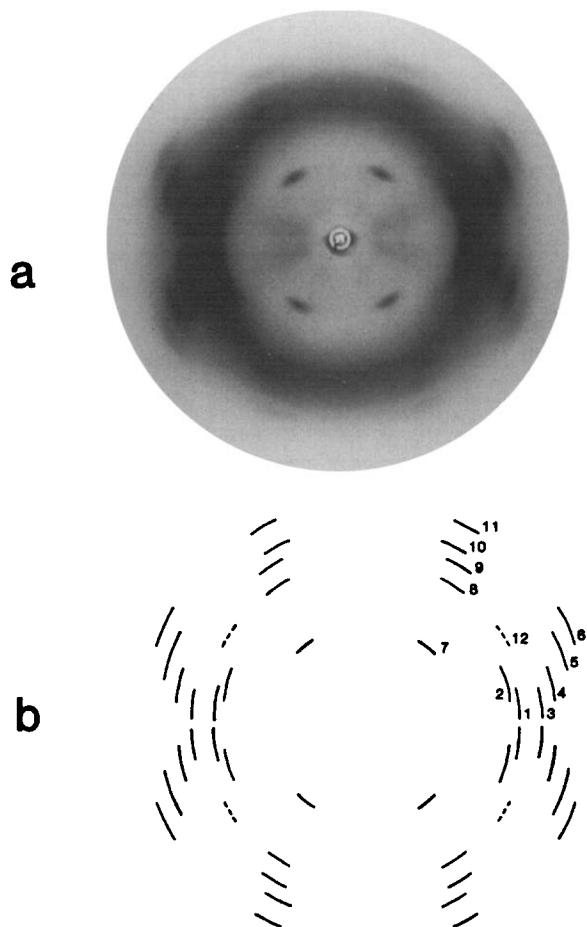


Figure 1 (a) X-ray diffraction photograph for MDI/BDO/PTMA stretched 700% and annealed at 130°C for 7 d. (b) Schematic diagram of diffraction pattern with reflections numbered for reference. ----, Reflection no. 12 due to the contracted form of poly(MDI/BDO)

poly(MDI-BDO) has been obtained from the determination of the crystal structures of diphenylmethane-urethane model compounds. *Figure 2* shows the structure of polymer proposed by Blackwell and Gardner¹¹ based on that of methanol capped MDI. They suggested that the monomer units in the polymer would probably be stacked and hydrogen bonded in a manner similar to that seen in the model compound. If these are then linked by butanediol units arranged in a planar zigzag conformation, then the dimer repeat is consistent with the fibre repeat ($c = 38 \text{ \AA}$) determined from the fibre diagram. The approximate unit cell dimensions predicted from this model are $a = 5.2$, $b = 4.8$, $c = 35.0 \text{ \AA}$, $\alpha = 115$, $\beta = 121$ and $\gamma = 85^\circ$. Subsequent conformational analysis¹² predicted a more extended chain with $c = 38 \text{ \AA}$, but which would still pack in the manner shown in *Figure 2*. Further confirmation of the proposed packing came from the determination of the structure of diphenylmethane 4-monoisocyanate capped butanediol^{10,13}, which was found to be almost superimposable on *Figure 2*. A survey of the structures of a number of analogous model compounds showed that fibre repeats ranging from 33.1 to 39.1 \AA could be achieved depending on the phenyl-urethane torsion angles¹⁴.

In the present paper we describe the manipulation of digital data obtained from two-dimensional densitometer scans of the X-ray and electron diffraction films in order to obtain better resolution of the Bragg reflections. Based on the combined X-ray and electron diffraction

data, a new unit cell for the fully extended form of poly(MDI-BDO) has been obtained.

EXPERIMENTAL

X-ray diffraction

The polyurethane elastomer samples used for the X-ray diffraction studies were prepared from melt pressed sheets of a bulk polymerized MDI/BDO/poly(tetramethylene adipate) (PTMA) ($M_n = 2000$) in a 7/6/1 molar ratio. The polymer was generously provided by Dr C. S. Schollenberger of B.F. Goodrich Co., Brecksville, Ohio. The films were oriented by stretching 700% and annealed in air at 130°C for 7 d. The diffraction patterns were recorded on Kodak Def-5 diffraction film using pin hole collimation of $\text{CuK}\alpha$ X-ray radiation. The specimen to film distance was determined by dusting the samples with CaF_2 powder.

Electron diffraction

The polyurethane system studied by electron microscopy was a solution polymerized sample of MDI/BDO/poly(propylene oxide) end-capped with ethylene oxide ($M_n = 2000$) containing 77% hard segment by weight. Oriented thin films were prepared from solution cast films of the polymer by hot drawing at 90°C. The films were then annealed at 160°C for 2-6 hours under N_2 in a Mettler hot stage.

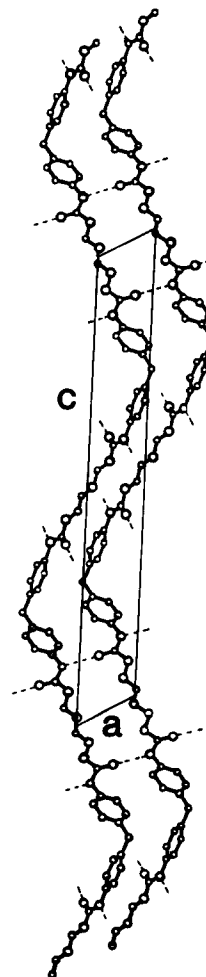


Figure 2 Projection of the structure of poly(MDI/BDO) proposed by Blackwell and Gardner¹¹

Densitometry

The diffraction data were digitized by two-dimensional scans of the films on an Optronix P-1000 rotational drum densitometer. The stepping raster and apertures were set at 100 μm . The digital data were manipulated by using a series of programs written by Fraser and colleagues^{15,16} of CSIRO, Parkville, Victoria, Australia, and modified by Dr K. H. Gardner of the du Pont Co., Wilmington, DE, USA. The centre of the film and the angle between the fibre axis and the main beam were determined using an interactive two-dimensional refinement routine. The data were also transformed from flat plate geometry to cylindrical reciprocal coordinates to facilitate indexing of the reflections.

RESULTS AND DISCUSSION

Background scatter by the non-crystalline regions (the soft segments and the amorphous fraction of the hard segments) tends to obscure some of the Bragg reflections and makes it difficult to determine their positions accurately. A minimum isotropic background was estimated by taking radial scans from the centre through regions where there were no reflections. This radial background is shown in *Figure 3*, and was subtracted from the diffraction pattern, resulting in the 'corrected' pattern shown in *Figure 4*. Note that significant diffuse scatter remains in the equatorial region at $d=4.5 \text{ \AA}$, presumably due to the fact that there is orientation of the non-crystalline regions, i.e. the background is not isotropic. Nevertheless, the Bragg reflections are more clearly resolved than in *Figure 1a*. The d spacings were determined from the peak maxima and are listed in *Table 1*, where the reflections are numbered for reference in the text.

Indexing of the reflections in *Figure 4* is assisted by replotting the data in R, Z space, where R and Z are the radial and axial coordinates in reciprocal space. This assists in determining the l index where c is large and the layer lines are relatively close, as in the case here. The R, Z plot in *Figure 5* is the average of the data in the upper left and right quadrants in *Figure 4*. Superimposed in *Figure 5* are layer lines for a repeat of

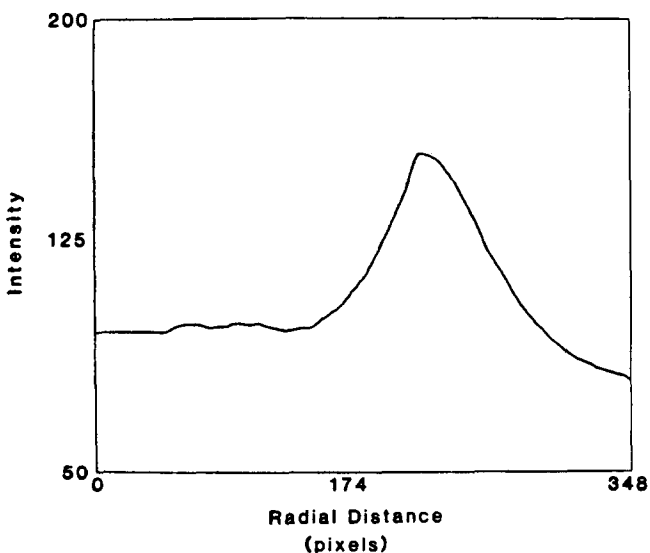


Figure 3 Average radial background for MDI/BDO/PTMA diffraction pattern used to subtract the isotropic non-crystalline background

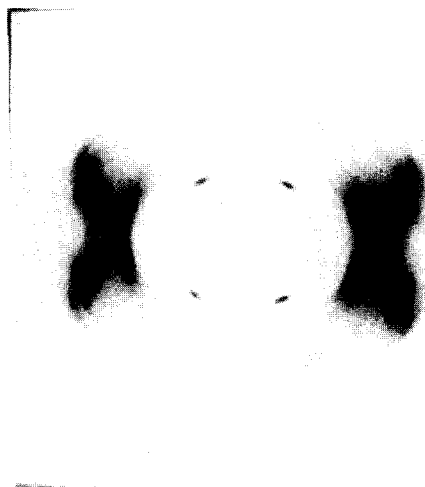


Figure 4 Digital intensity image of X-ray diffraction photograph corrected for isotropic background

Table 1 Observed and calculated d -spacings

No.	h	k	l	$d_{\text{obs.}} (\text{\AA})$	$d_{\text{calc.}} (\text{\AA})$
1	$\bar{1}$	0	1	4.84	4.89
	0	$\bar{1}$	1		4.90
2	0	$\bar{1}$	2	5.13	5.13
3	0	1	1	4.26	4.24
4	0	1	2	3.89	3.90
5	1	0	3	3.54	3.54
	$\bar{1}$	1	4		3.50
6	0	1	4	3.29	3.29
	$\bar{1}$	1	5		3.31
7	0	0	4	7.65	7.60
8	$\bar{1}$	0	7	4.53	4.51
9	0	$\bar{1}$	8	4.08	4.04
10	$\bar{1}$	0	9	3.80	3.81
11	0	$\bar{1}$	10	3.41	3.41
12	Assigned to second polymorphic form			4.60	
13	0	0	6	5.10	5.07
14	0	0	10	3.05	3.04
15	$\bar{1}$	$\bar{1}$	16	2.42	2.41
16	$\bar{1}$	$\bar{1}$	18	2.15	2.15
17	$\bar{1}$	$\bar{1}$	20	1.93	1.92
18	$\bar{1}$	$\bar{1}$	22	1.73	1.73
19	$\bar{2}$	0	15	2.18	2.16
20	$\bar{2}$	0	17	1.99	1.99
21	$\bar{2}$	1	12	2.02	2.03
22	$\bar{1}$	1	7	2.96	2.94

The standard deviation between the observed and calculated data is 0.022 for unit cell

$c = 38.68 \text{ \AA}$, assuming that c is parallel to the direction of draw. It can be seen, for example, that reflection no. 6 at $d = 3.29 \text{ \AA}$ lies on or near the fifth layer line, rather than the fourth layer line as originally proposed⁴. It is also interesting that the centres of reflections nos 3, 4 and 5 lie between the nearest layer lines.

Figure 6a shows the electron diffraction pattern obtained with the plane of the film specimen perpendicular to the beam. *Figures 6b* and *c* are the electron diffraction patterns for the same specimen after it had been rotated 40° about axes corresponding to the equator and meridian, respectively, in *Figure 6a*. An isotropic background was subtracted from each pattern in the same way as for the X-ray data, resulting in the 'corrected' data shown in *Figure 7a-c*. The d spacings of the observed reflections are given in *Table 1*. The specimens are shown to have non-fibre texture in that reflections nos 7, 13 and

14 are not seen for zero tilt but are only obtained after a 40° tilt about the equator (Figure 7b). Similarly, generation of reflections nos 1–4 requires a 40° tilt about the fibre axis (Figure 7c). Further discussion of the texture of poly(MDI-BDO) crystallites in the specimens prepared for electron microscopy is given elsewhere by Briber and Thomas⁷. A composite schematic showing the reflections seen on all the patterns is shown in Figure 7d and contains a total of 22 reflections. Most of the additional reflections not seen in the X-ray patterns are at low d spacings ($d < 3 \text{ \AA}$). The appearance of 00 l reflections when the film is tilted by 40° about the equator is compatible with a staggered packing of the chains as in the triclinic structure shown in Figure 2. The observed d spacings can be indexed by a triclinic unit cell with least squares refined dimensions $a = 5.33$, $b = 5.26$, $c = 38.68 \text{ \AA}$, $\alpha = 113.6$, $\beta = 116.0$, $\gamma = 94.4^\circ$. The observed and calculated d spacings are compared in Table 1, and in all cases the agreement is within experimental error. The calculated density is 1.33 g cm^{-3} , which is in good agreement with the reported values of $1.25\text{--}1.35 \text{ g cm}^{-3}$, and the dimensions are in accord with predictions from model compound and conformational analyses.

As mentioned previously, the observed reflections do not occur on straight layer lines. We considered the

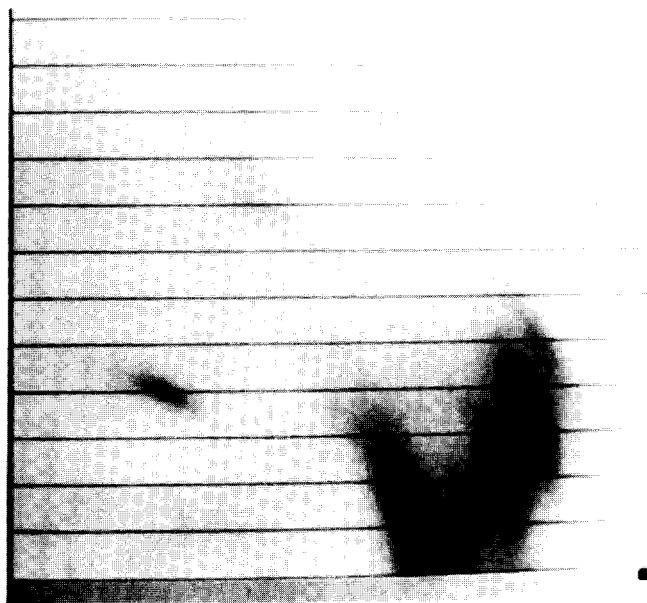


Figure 5 One quadrant of MDI/BDO/PTMA X-ray diffraction pattern transferred to reciprocal cylindrical coordinates

possibility that the observed reflections are composites of reflections with approximately the same d -spacing but different l indices. Such an explanation could be invoked for reflection no. 5, which could be a combination of the 103 and $\bar{1}14$ reflections, but not for reflections nos 3 and 4. A more likely explanation of the non-linearity is that the c axis of the unit cell is not parallel to the direction of draw. Such tilting of the chains relative to the fibre axis has been reported for some other triclinic polymer system, notably poly(ethylene terephthalate)¹⁷.

The tilt of the unit cell is defined by ϕ , the angle between the c axis and the direction of draw, and ψ , the angle between the original ac plane and the plane containing c and the direction of draw. These angles were refined to obtain the best least squares fit between the observed and calculated Z coordinates for the reflections. The function minimized is

$$r = (\sum_i (Z_{oi} - Z_{ci})^2 / \sum_i Z_{oi}^2)^{1/2}$$

where the subscripts oi and ci designate observed and calculated Z coordinates for the i th reflection. The final model had $r = 0.012$ and the refined parameters were $\phi = 2.5^\circ$ and $\psi = 50^\circ$, which corresponds to a tilt of the c axis of 2.5° approximately in the $\bar{1}11$ plane ($\psi = 49.12^\circ$ would place the c axis exactly in the $\bar{1}11$ plane). The observed and calculated Z coordinates are shown in Table 2, and a qualitative picture of the agreement between observed and calculated position is given in Figure 8. A schematic of the tilted unit cell is Figure 9. Tilting of the unit cell relative to the direction of draw has been found to be quite common for triclinic systems, and can be rationalized by the asymmetry of the chains

Table 2 Observed and calculated axial coordinates in reciprocal space

No.	h	k	l	$Z_c (10^{-3} \text{ \AA}^{-1})$	$Z_o (10^{-3} \text{ \AA}^{-1})$
1	$\bar{1}$	0	1	18.5	20.6
	0	$\bar{1}$	1	20.3	
2	0	$\bar{1}$	2	46.0	46.4
3	0	1	1	34.3	37.4
4	0	1	2	61.1	58.6
5	1	0	3	88.4	86.0
	$\bar{1}$	1	4	105.6	
6	0	1	4	114.0	
	$\bar{1}$	1	5	132.4	129.5
7	0	0	4	106.9	106.5
8	$\bar{1}$	0	7	181.0	182.8
9	0	$\bar{1}$	8	206.3	208.7
10	$\bar{1}$	0	9	232.2	230.7
11	0	$\bar{1}$	10	259.6	258.4

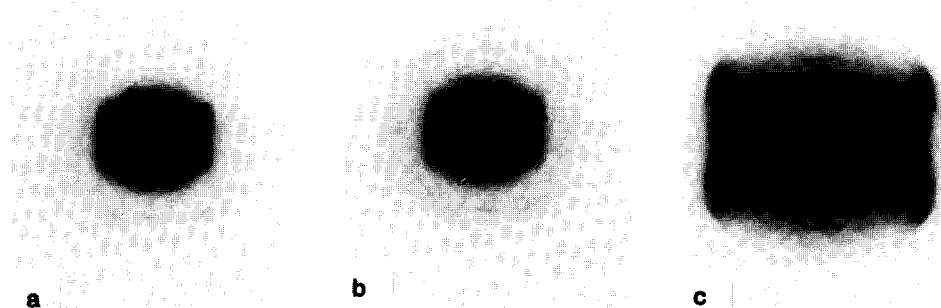


Figure 6 Electron diffraction patterns from oriented spherulites of MDI/BDO/PPO-PEO: (a) plane of specimen perpendicular to the beam; (b) rotated 40° about the equator (originals provided by Dr R. M. Briber and Dr E. L. Thomas of the University of Massachusetts); (c) rotated 40° about the meridian

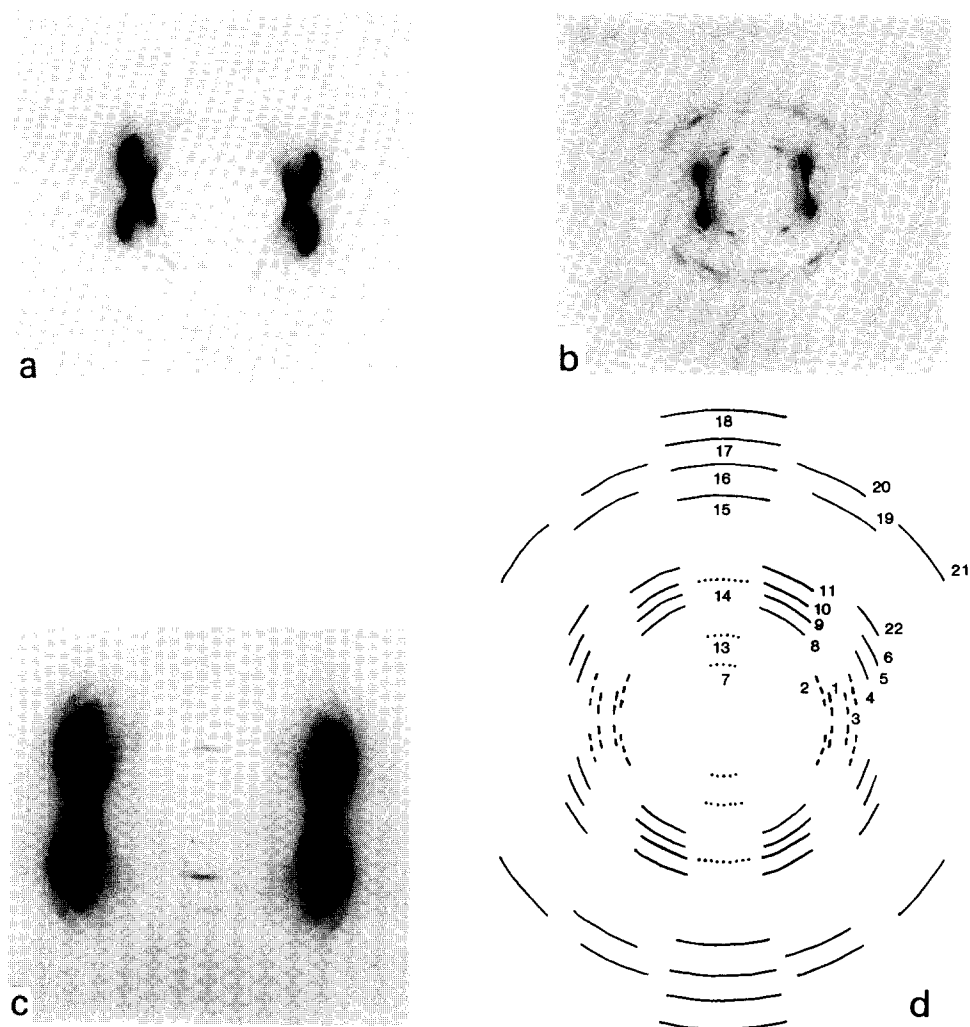


Figure 7 Digital intensity image of electron diffraction patterns corrected for isotropic background: (a) plane of specimen perpendicular to the beam; (b) 40° tilt about the equator; (c) 40° tilt about the fibre axis. (d) Composite schematic diagram of all the electron diffraction patterns: —, reflections observed in untilted pattern are indicated by solid line; ---, additional reflections observed after 40° tilt about the fibre axis; ···, reflections observed after 40° tilt about equator

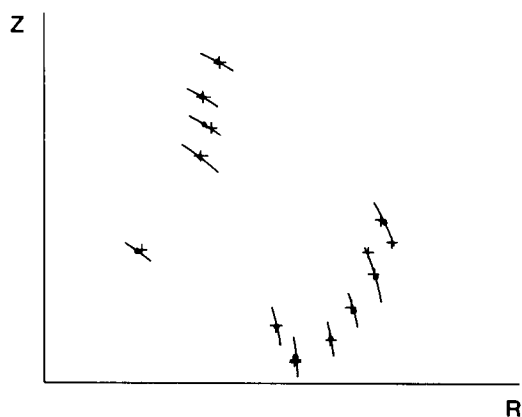


Figure 8 Schematic R, Z map for the X-ray data. The arcs represent the observed reflections with their centres indicated by ●. The layer lines are those predicted for the proposed unit cell with c parallel to the direction of draw. The calculated positions for a structure in which c is tilted by 2.5° approximately in the $\bar{1}11$ plane are shown by +

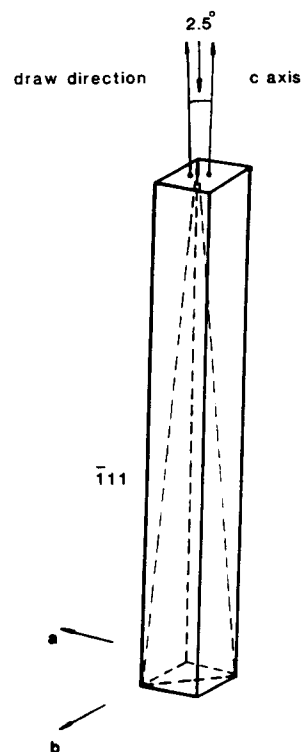


Figure 9 Proposed unit cell and direction of tilt

that emerge from the top and bottom of the crystalline lamellae, resulting from staggering of the molecules to form a hydrogen bonded network.

A future paper will describe refinement of the poly-(MDI-BDO) structure based on the X-ray intensity data.

ACKNOWLEDGEMENT

This work was supported by NSF through grant no. DMR 84-17525 (at Case Western Reserve University) and by grant no. CBT 85-12120 (at the University of Massachusetts).

REFERENCES

- 1 Cooper, S. L. and Tobolsky, A. V. *J. Appl. Polym. Sci.* 1966, **10**, 1837
- 2 Bonart, R. *J. Macromol. Sci. Phys.* 1968, **2**, 115
- 3 Wilkes, C. W. and Yusek, C. J. *J. Macromol. Sci. Phys.* 1973, **7**, 157
- 4 Blackwell, J. and Ross, M. *J. Polym. Sci., Polym. Lett.* 1979, **17**, 447
- 5 Blackwell, J., Nagarajan, M. R. and Hoitink, T. *Polymer* 1981, **22**, 1534
- 6 Blackwell, J. and Lee, C. D. *J. Polym. Sci. Polym. Phys.* 1984, **22**, 759
- 7 Briber, R. M. and Thomas, E. L. *J. Macromol. Sci. Phys.* 1983, **B22**, 509
- 8 Briber, R. M. and Thomas, E. L. *J. Polym. Sci. Polym. Phys.* 1985, **23**, 1915
- 9 Born, L., Crone, J., Hesse, H., Muller, E. H. and Wolf, K. H. *J. Polym. Sci. Polym. Phys.* 1984, **22**, 163
- 10 Leung, L. M. and Koberstein, J. T. *J. Polym. Sci. Polym. Phys.* 1985, **23**, 1883
- 11 Blackwell, J. and Gardner, K. H. *Polymer* 1979, **20**, 13
- 12 Blackwell, J. and Nagarajan, M. R. *Polymer* 1981, **22**, 202
- 13 Born, L., Hesse, H., Crone, J. and Wolf, K. H. *Colloid Polym. Sci.* 1982, **260**, 819
- 14 Blackwell, J., Quay, J. R., Nagarajan, M. R., Born, L. and Hesse, H. *J. Polym. Sci. Polym. Phys.* 1984, **22**, 1247
- 15 Fraser, R. D. B., MacRae, T. P., Miller, A. and Rowlands, R. J. *J. Appl. Cryst.* 1976, **9**, 81
- 16 Fraser, R. D. B., Suzuki, E. and MacRae, T. P. Computer analysis of X-ray diffraction patterns, in 'Structure of Crystalline Polymers', (Ed. T. H. Hall), Elsevier Applied Science, London, 1984
- 17 Daubeny, R. de P., Bunn, C. W. and Brown, C. J. *Proc. Roy. Soc. Lond.* 1954, **A226**, 531